IOP Publishing Journal of Physics B: Atomic, Molecular and Optical Physics

J. Phys. B: At. Mol. Opt. Phys. **40** (2007) 1211–1223 doi:10.1088/0953-4075/40/6/011

Electron collision with the HCN and HNC molecules using the *R*-matrix method

Hemal N Varambhia and Jonathan Tennyson

Department of Physics and Astronomy, University College London, Gower St., London WC1E 6BT, UK

Received 24 November 2006, in final form 11 February 2007
Published 5 March 2007
Online at stacks.iop.org/JPhysB/40/1211

Abstract

The linear isomers HCN and HNC are both well known astrophysically. Electron collision calculations are presented using a 24 target state close-coupling expansion and a variety of models. All of these confirm the presence of the previously identified $^2\Pi$ HCN anion shape resonance, although it is found that this resonance is somewhat narrower than suggested by previous calculations. HNC is also predicted to have $^2\Pi$ anion shape resonance at a similar energy but somewhat narrower than its HCN^- counterpart. Furthermore HNC also supports two narrow Feshbach resonances of $^2\Sigma^+$ and $^2\Delta$ symmetry. Results are presented for the electron impact electronic excitation of both molecules.

(Some figures in this article are in colour only in the electronic version)

1. Introduction

The isomers hydrogen cyanide (HCN) and hydrogen isocyanide (HNC) are very polar linear species. Despite the fact that HCN is the significantly more stable form, both are well known in the cold interstellar medium (ISM) where concentrations of HNC often exceed those of HCN (Hirota *et al* 1998). More recently HNC has also been identified in the spectra of cool carbon stars where HCN is well known (Harris *et al* 2003).

Electron collisions with these two molecules are of potential interest to the astrophysical community. Their large dipole moments, both about 3 Debye, means that cross-sections for electron collisions can be expected to be large. Recently calculated electron collision cross-sections for the iso electronic molecular ion HCO^+ have been used to measure electron densities in a shocked region of the ISM (Jimenez-Serra *et al* 2006). HCN and HNC are possible neutral candidates for similar studies. Indeed electron impact excitation of HCN has been shown to be important in cometary tails (Lovell *et al* 2004).

Electron collisions with HCN have been studied by a number of workers. Srivastava *et al* (1978), Edard *et al* (1990) and Burrow *et al* (1992) all performed experiments which showed the existence of a shape resonance of $^2\Pi$ symmetry. Edard *et al* also obtained absolute

cross-sections by comparing, in the same experimental conditions, the electron loss spectrum of the isoelectronic species N_2. However, none of these studies considered electron impact electronic excitation of HCN.

Theoretically electron collisions with HCN were extensively studied by Jain and Norcross (1985, 1986) using a variety of one state models. They also reported finding a shape resonance of $^2\Pi$ symmetry and found that its calculated position and width were sensitive to the treatment of polarization in the calculation. The work of Jain and Norcross remains the most comprehensive theoretical treatment of this problem to date.

To our knowledge there has been no previous work, either experimental or theoretical, on electron collisions with HNC. However, we note that HCN and HNC are each predicted to support an extremely weakly (dipole) bound anion state (Skurski *et al* 2001).

In this work we report simultaneous coupled states calculations on electron collisions with both HCN and HNC. This allows not only the study of possible resonances in these collision systems but also the consideration of other properties such as electronic excitation. The following section gives a brief overview of the *R*-matrix method used for these calculations; it is followed by details of the theoretical models tested and our results.

2. The *R*-matrix method

The UK polyatomic *R*-matrix method (Morgan *et al* 1997, 1998) has been applied to a wide variety of diatomic and polyatomic molecules including polar polyatomic molecules CF_3 (Rozum *et al* 2003) and NH_3 (Munjal and Baluja 2006). The development of the underlying theory is well documented (Burke and Berrington 1993, Burke and Tennyson 2005).

The *R*-matrix method is based on the splitting of co-ordinate space into an inner and outer region, separated by a spherical boundary, here of radius $r = 10a_0$, whose centre coincides with the centre of mass of the molecule. The boundary is such that the molecular electron cloud is fully contained within the sphere. Interaction between the scattering electron and target have qualitatively different properties in the two regions. In the inner region the scattering electron is inside the molecular charge cloud so exchange and electron–electron correlation interactions are important. This anionic complex behaves in a similar way to a molecular bound state and consequently configuration interaction (CI) is used in the same manner as for molecular bound state calculations. In the outer region however, exchange and correlation are negligible and only long-range multi-polar interactions between the target and scattering electrons need to be considered. In this region the scattering problem may be reduced to solving coupled second-order differential equations which in practice is done by propagating the *R*-matrix and asymptotic expansion of the solution (Morgan *et al* 1998).

In the inner region the scattering wavefunction Ψ_k^{N+1} is expressed as a close-coupling (CC) expansion:

$$\Psi_k^{N+1} = A \sum_i \psi_i^N(x_1, x_2, \ldots, x_n) \sum_j \kappa_j(x_{N+1}) a_{ijk} + \sum_l \chi_l(x_1, x_2, \ldots, x_{N+1}) b_{lk}, \tag{1}$$

where A is the anti-symmetrization operator and $\mathrm{x}_i = \mathbf{r}_i\sigma_i$ is the spin-space co-ordinate of the ith electron, ψ_i^N is the target wavefunction and κ_j is the jth continuum orbital spin coupled with the scattering electron. The expansion coefficients are such that they diagonalize the inner region Hamiltonian to which a Bloch operator needs to be added so as to ensure this Hamiltonian remains Hermitian on the boundary. The first summation yields the target and continuum configurations and the second runs over the χ_l which are configurations in which all electrons are placed in target molecular orbitals. These configurations are square integrable and often referred to as L^2 functions.

The target wavefunctions are usually determined from a CI calculation, in which a wavefunction is written as a linear combination of CSFs (configuration state functions)

$$\psi_k^N = \sum_i c_{ki}\phi_i^N, \tag{2}$$

where the expansion coefficients c_{ki} are such that they diagonalize the target Hamiltonian matrix due to the basis of the CSFs. The target molecular orbitals are constructed from Gaussian-type orbitals (GTOs). The continuum orbitals used here are those of Faure *et al* (2002) and include up to g ($l = 4$) orbitals; unlike those used in the electron-diatomic molecule code (Tennyson and Morgan 1999), these orbitals have no particular boundary conditions. The advantage of using Gaussian-type orbitals is that infinite integrals are then evaluated exactly. The integrals are actually required over the inner region, hence the tail integrals representing the outer region contribution have to be subtracted. This can be done efficiently using property integrals for the short-range GTOs (see Morgan *et al* (1997) for details).

In this work complete active space (CAS) CI target wavefunctions are employed. In this model the target molecular orbitals included in the scattering calculation are divided into core (which are fully occupied in all configurations), active and virtual orbitals. In the latter two orbital spaces electrons are allowed to undergo excitation to orbitals of higher energy by following a prescription which retains the balance between target and scattering calculations (Tennyson 1996).

While most of the calculations reported below used the standard UK molecular *R*-matrix codes (Morgan *et al* 1998), we took the opportunity to use the Quantemol-N scattering software (Tennyson *et al* 2006). Quantemol-N is an expert system which runs the *R*-matrix codes with a minimal set of input parameters. It is black box software in much the same spirit as the Gaussian package (Frisch *et al* 2004). It was our intention to compare the results of the target and scattering model *automatically generated* by the software with that of our own. The defaults which most affect the calculations below are that the orbitals for the CAS and the number of target states included in the close-coupling equation are chosen on energy grounds. Unless stated otherwise these default values were used in all Quantemol-N calculations.

All the calculations reported here were carried out in the fixed nuclei approximation.

3. HCN and HNC target calculation

There have been a number of previous studies on the electronically excited states of HCN (Schwenzer *et al* 1974, Nayak *et al* 2005). The most comprehensive appears to be the recent study by Nayak *et al* (2005) who aimed at characterizing the excited triplet states of HCN. Their transition energies were computed using coupled-cluster-based linear response theory. Unfortunately they only report adiabatic excitation energies whereas for our calculations the higher vertical excitation energies are required. Experimentally obtained adiabatic excitation energies are only available for a rather smaller set of states (Herzberg 1966, Krishnamachari S and Venkatsubramanian 1986).

Schwenzer *et al* (1975) provide a rare theoretical study of electronically excited HNC. They too only report adiabatic excitation energies. As their calculations used only a double zeta basis set and single excitation CI, their results cannot be regarded as definitive.

In the present study, experimental equilibrium geometries (NIST 2005) were used for all calculations on both molecules. The ground-state electronic configuration of HCN and its isomer in the $C_{\infty v}$ symmetry is $1\sigma^2 2\sigma^2 3\sigma^2 4\sigma^2 5\sigma^2 1\pi^4$, hence both ground states have symmetry $^1\Sigma^+$. However, since the polyatomic code only supports Abelian point groups

(Morgan *et al* 1998), all calculations were performed in the C_{2v} sub-group, in which the ground state electron configuration is $1a_1^2\ 2a_1^2\ 3a_1^2\ 4a_1^2\ 5a_1^2\ 1b_1^2\ 1b_2^2$.

A number of Gaussian-type orbital (GTO) target basis sets of double zeta or better quality were tested: 6-31G, 6-31G* and 6-311G. In each case a Hartree–Fock self-consistent field (SCF) calculation was performed to obtain initial occupied and virtual orbitals. In the subsequent configuration interaction (CI) calculations the $1a_1$ and $2a_1$ orbitals (hence four electrons) were frozen. The remaining ten electrons were allowed to move freely among the $3a_1$, $4a_1$, $5a_1$, $6a_1$, $1b_1$, $2b_1$, $1b_2$ and $2b_2$ active orbitals.

For calculations using Quantemol-N the basis set 6-31G was adopted. This software generates its own complete active space, subject to the analysis of the molecular orbital energies obtained from its SCF calculation. The complete active space used by the software for the CI calculation was slightly larger than as ours:

$$(1a_1 2a_1)^4 (3a_1 4a_1 5a_1 6a_1 7a_1 1b_1 2b_1 1b_2 2b_2)^{10} \tag{3}$$

whereas for HNC the Quantemol-N CAS and that of this work coincided.

One problem with representing the target states in a scattering calculation is the need to use a single orbital set for all states. It is possible to further improve the quality of the target wavefunctions by constructing weighted pseudo natural orbitals (NOs). In all NO calculations we used the first five lowest target states ($^1A_1$, $^3A_1$, $^3A_2$, $^3B_1$, $^3B_2$). Each target state is represented by a CI wavefunction. All possible single and double excitation to unoccupied virtual orbitals were included. In order to be able to incorporate the double excitations however, it was necessary to freeze eight electrons (the 1 s and 2 s electrons of C and N). For both HCN and HNC the weighting coefficients for the averaging procedure on the density matrix were 5.75, 1.5, 1.5, 1.5, 1.5 for $^1A_1$, $^3A_1$, $^3A_2$, $^3B_1$, $^3B_2$, respectively. Care needs to be taken in choosing a target model for the natural orbitals calculation. If not treated in exactly the same fashion, the degeneracy between orbitals (e.g., those of b_1 and b_2 symmetry) can be easily broken.

3.1. HCN target model results

Table 1 reports HCN vertical excitation energies (those below the first ionization energy), the absolute ground state energy and dipole moments obtained from the target models discussed above. We compare our results to the adiabatic data of (Nayak *et al* 2005) and the experimental results of Herzberg (1966).

It should be noted that whereas we chose to compute vertical excitation energies for 24 states (three states per irreducible representation per spin multiplicity), by default Quantemol-N only considers those states energies whose vertical excitation energies are less than 10 eV.

3.2. HNC target model results

Results of our HNC calculations are summarized in table 2 where they are compared with the cruder study of Schwenzer *et al* (1975). We know of no experimental measurement of the excitation energy. The calculated ground state dipole moments are all close to the observed value of −1.20 au (NIST 2005).

The data obtained from Quantemol-N and the equivalent *R*-matrix calculation are in agreement because, as mentioned previously, the target models used are the same. Note that we find the ground state of HNC lies 0.73 eV above that of HCN, close to the accurate value of 0.65 eV obtained by Van Mourik *et al* (2001).

Table 1. HCN vertical excitation energies, in eV, calculated in this work compared to the published adiabatic excitation energies. Also given are the absolute energy of the ground state, in Hartree, the ground state dipole moment and the number of configurations generated by our CAS CI calculation. State designations are give in $C_{\infty v}$ (C_{2v}) symmetry.

Target State	N	6-31G	6-311G	6-31G*	6-31G+NO	Quantemol-N	CC[a]	Experiment[b]
$X\,^1\Sigma^+$ ($^1A_1$)	328	−92.902	−92.911	−92.939	−92.939	−92.9109		
$1\,^3\Sigma^+$ ($^3A_1$)	360	6.87	7.04	6.90	6.63	6.85	6.13	
$1\,^3\Delta$ ($^3A_1$, $^3A_2$)	384	8.03	8.04	7.98	7.96	8.05	7.00	
$1\,^3\Pi$ ($^3B_1$, $^3B_2$)	384	8.50	8.61	8.89	8.53	8.50	4.44	8.53[c]
$1\,^3\Sigma^-$ ($^3A_2$)	384	8.72	8.72	8.67	8.97		5.47	
$1\,^1\Sigma^-$ ($^1A_2$)	272	9.09	9.02	8.98	9.23	9.15	6.48	6.48
$1\,^1\Delta$ ($^1A_1$, $^1A_2$)	272	9.41	9.30	9.26	9.82		6.93	6.77
$1\,^1\Pi$ ($^1B_1$, $^1B_2$)	288	9.84	9.91	10.18	10.04	9.83	8.10	8.10
$2\,^3\Pi$ ($^3B_1$, $^3B_2$)	384	11.87	11.69	11.70			6.81	
$2\,^1\Pi$ ($^1B_1$, $^1B_2$)	288	12.17	11.80	11.98			8.64	8.88
$2\,^3\Sigma^+$ ($^3A_1$)	360	12.40	12.16	12.61				
$2\,^1\Sigma^+$ ($^1A_1$)	328	12.53	12.24	12.76			7.79	
$3\,^3\Pi$ ($^3B_1$, $^3B_2$)	384						7.47	
μ/au		−1.19	−1.21	−1.17	−1.13	−1.193	−1.26[d]	−1.172[e]

[a] Coupled Cluster results from Nayak *et al* (2005).
[b] Herzberg (1966).
[c] Krishnamachari S and Venkatsubramanian (1986).
[d] Jain and Norcross (1985).
[e] NIST (2005).

Table 2. HNC vertical excitation energies, in eV, calculated in this work compared to the published adiabatic excitation energies. Also given are the absolute energy of the ground state, in Hartree, and the calculated ground state dipole moment. Since HCN and HNC are isoelectronic the number of configurations for each symmetry is the same as those given in table 1.

Target State	6-31G	6-311G	6-31G*	6-31G+NO	Quantemol-N	Theory[a]
$X\,^1\Sigma^+$ ($^1A_1$)	−92.875	−92.892	−92.909	−92.897	−92.875	
$1\,^3\Pi$ ($^3B_1$, $^3B_2$)	6.16	6.40	6.48	6.20	6.16	
$1\,^3\Sigma^+$ ($^3A_1$)	7.88	7.94	7.91	7.45	7.88	4.46
$1\,^3\Delta$ ($^3A_1$, $^3A_2$)	8.61	8.63	8.65	8.36	8.61	4.60
$1\,^3\Sigma^-$ ($^3A_2$)	8.98	8.99	9.06	8.94		5.22
$1\,^1\Pi$ ($^1B_1$, $^1B_2$)	9.01	9.08	9.313	9.18	9.01	7.34
$1\,^1\Sigma^-$ ($^1A_2$)	9.26	9.25	9.310	9.20	9.26	4.95
$1\,^1\Delta$ ($^1A_1$, $^1A_2$)	9.27	9.26	9.35	9.38		5.51
$2\,^3\Sigma^+$ ($^3A_1$)	10.52	10.23	10.66	13.31		5.44
$2\,^1\Sigma^+$ ($^1A_1$)	10.56	10.25	10.71	13.42		6.22
$2\,^3\Pi$ ($^3B_1$, $^3B_2$)	11.85	11.46	11.67	13.83		
$2\,^1\Pi$ ($^1B_1$, $^1B_2$)	12.23	11.71	12.05			8.50
$2\,^3\Sigma^-$ ($^3A_2$)						5.96
$2\,^1\Sigma^-$ ($^1A_2$)						8.17
$3\,^3\Sigma^-$ ($^3A_2$)						6.09
μ/au	−1.15	−1.21	−1.16	−1.146	−1.15	

[a] Schwenzer *et al* (1975).

4. HCN and HNC scattering calculation

As the calculation of resonances involves the variational principle, 24 target states were included in the close-coupling expansion in order to keep the expected resonance position as

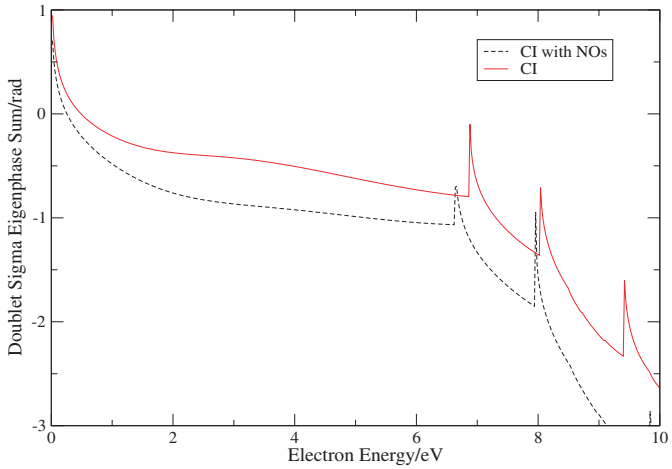

Figure 1. Comparison of HCN eigenphase sum curve $^2\Sigma^+$ symmetry for calculations with a 6-31G target basis.

low as possible, and to avoid any pseudo resonances which may otherwise appear when too few states are included in the expansion. Calculations were performed for the (C_{2v}) scattering symmetries $^2A_1$, $^2B_1$, $^2B_2$ and $^2A_2$. The continuum GTOs were symmetrically (Lowden) orthogonalized among themselves and then Schmidt orthogonalized to the target orbitals. Only those continuum orbitals with an eigenvalue greater than 2×10^{-7} in the symmetric orthogonalization were retained. One virtual orbital was chosen for each symmetry where target orbitals were available to do so (see section 2). The scattering model used by Quantemol-N was the same as the above except that only those states with vertical excitation energies lower than 10 eV were included in the close-coupling expansion.

Convergence of the polarization interactions in methods based on close-coupling expansions remains an issue (Gil *et al* 1994, Gorfinkiel and Tennyson 2004). For this reason we tried calculations which not only differed in the target parameters, i.e. basis set and orbitals, but also tested models which differed in the way the virtual orbitals are used. Calculations on electron collisions with the isoelectronic CO molecule (Salvini *et al* 1984) showed significant dependence on how the virtuals were treated. Our initial calculations contracted CSFs in which the scattering electron occupied a virtual orbital with the target CI (see Tennyson (1996), meaning that such CSFs are treated as part of the first sum in equation (1). However, to allow for increased polarizability, which appears to be systematically underestimated in previous calculations (Gorfinkiel and Tennyson 2004, Gorfinkiel and Tennyson 2005), we also tested models which use a separable treatment of virtual and continuum orbitals. In this treatment CSFs are not contracted, thus moving them to the second, or L^2, summation in equation (1).

Resonance parameters were obtained by fitting the eigenphase sum curve to a Breit-Wigner profile (Tennyson and Noble 1984).

4.1. HCN resonance parameters

The eigenphase curve for $^2\Sigma^+$ scattering symmetry given in figure 1 shows a sharp upturn as the scattering energy goes to zero—the behaviour one would expect by Levinson's theorem

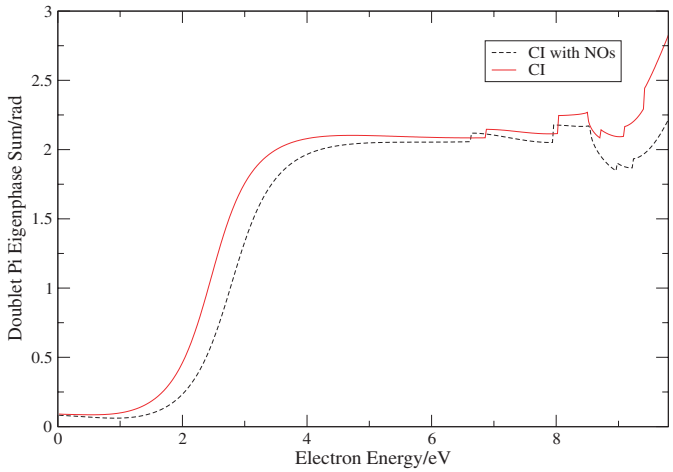

Figure 2. Comparison of HCN eigenphase sum curve $^2\Pi$ symmetry for calculations with a 6-31G target basis.

Table 3. HCN resonance parameters in eV as a function of model.

$^2\Pi$	6-31G	6-31G[a]	6-311G	6-31G*	6-31G+NO[a]	Quantemol-N	Theory[b]	Experiment[c]
E_r	2.83	2.46	2.84	3.14	2.79	3.27	2.56–2.80	2.26
Γ_r	1.34	1.14	1.49	1.59	1.22	1.64	1.78–2.40	

[a] Obtained using separate treatment of virtual and continuum orbitals.
[b] Jain and Norcross (1985).
[c] Burrow *et al* (1992).

for a system supporting a weakly bound state. The $^2\Sigma^+$ eigenphase for HNC shows a similar behaviour. We note however, that for HCN the $^2\Sigma^+$ eigenphase curve in figure 1 does not show any resonance features. The structure of the curve at energies below the first target excitation threshold, at about 6.8 eV, is very similar to the curve given by Jain and Norcross (1985). Figure 2 which presents the same data for the $^2\Pi$ symmetry shows the clear signature of a broad, low-energy resonance, also in agreement with the previous studies. For both scattering symmetries our eigenphases show considerable structure associated with the opening of new target electronic excitation channels above 6.8 eV; this structure is not present in Jain and Norcross's study since they used a 1-state approximation.

Table 3 summarizes the results we obtained for the position and width of the $^2\Pi$ resonance. These results show considerable sensitivity to the precise model used, with the position varying by more than 0.5 eV and the width by over 20% between different calculations. This behaviour is similar to that observed by Jain and Norcross (1985), for whom only results which explicitly included polarization effects are quoted. Unsurprisingly their static exchange results give resonances which are systematically broader and higher.

Our predicted resonances lie at very similar energies to those of Jain and Norcross (1985), the lowest being about 0.2 eV higher than the most precise experimental resonance energy position measurement of due to Burrow *et al* (1992). However, it should be noted this experiment measures the adiabatic resonance energy whereas the calculations are for the higher vertical energy.

Table 4. HNC shape resonance parameters in eV.

$^2\Pi$	6-31G	6-31G[a]	6-311G	6-31G*	6-31G+NO[a]	Quantemol-N
E_r	2.77	2.57	2.90	3.03	2.43	3.15
Γ_r	0.91	0.80	1.06	1.10	0.67	1.15

[a] Obtained using the separate treatment of continuum and virtual orbitals.

Table 5. HNC resonance parameters in eV.

$^2\Sigma^+$	6-31G	6-31G[a]	6-311G	6-31G*	6-31G+NO[a]	Quantemol-N
E_r		7.82	7.85		7.43	7.84
Γ_r		2.2×10^{-3}	3.0×10^{-3}		1.2×10^{-3}	9.6×10^{-4}
$^2\Delta$	6-31G	6-31G[a]	6-311G	6-31G*	6-31G+NO[a]	Quantemol-N
E_r		8.57		8.61	8.34	8.58
Γ_r		4.0×10^{-4}		5.5×10^{-4}	3.5×10^{-4}	3.4×10^{-4}

[a] Obtained using separate treatment of virtual and continuum orbitals.

The HCN $^2\Pi$ shape resonance is rather broad. However, all our calculations find it to be systematically narrower than the studies of Jain and Norcross (1985, 1986). A narrower resonance normally corresponds to an improved treatment of short-range polarization effects as this lowers the energy with a corresponding reduction in the phase space available for the continuum. Our widths, which are still greater than 1 eV, are consistent with the experimental finding (Burrow *et al* 1992) that the resonance is too broad to support any vibrational structure.

Finally we note that for HCN we found no evidence of any Feshbach resonances.

4.2. HNC resonance parameters

Our calculations clearly show that HNC also has a $^2\Pi$ symmetry shape resonance, the parameters for which are given in table 4 as a function of different models. Our calculations predict the position of the resonance to be very similar to the HCN $^2\Pi$ shape resonance; however they all suggest that the HNC resonance is narrow with a width only about 60% of that calculated for HCN.

The most notable difference in our scattering calculation on HNC compared to HCN is the appearance of a number of narrow resonances. These resonances, unlike the shape resonance found for both isomers, do not appear in all calculations but only those with an enhanced treatment of polarization. This behaviour is thus characteristic of Feshbach resonances which do not occur in calculations containing an inadequate treatment of polarization effects.

Table 5 gives parameters for the narrow $^2\Sigma^+$ and $^2\Delta$ symmetry resonances. Results absent from this table mean that the model did not predict a resonance. The resonance positions in the table appear to vary by nearly 0.5 eV. This is not actually a property of the scattering calculations but of the underlying representation of the target states. The $^2\Sigma^+$ and $^2\Delta$ resonances appears to be associated with the first excited $^3\Sigma^+$ and $^3\Delta$ states of HNC, respectively. In all cases our calculations find the resonance appears less than 0.1 eV below their respective parent state. The sensitivity in the resonance position is thus directly associated with the differences in target vertical excitation energies, see table 2. The correlation between which models (i.e., those with the uncontracted treatment of short-range

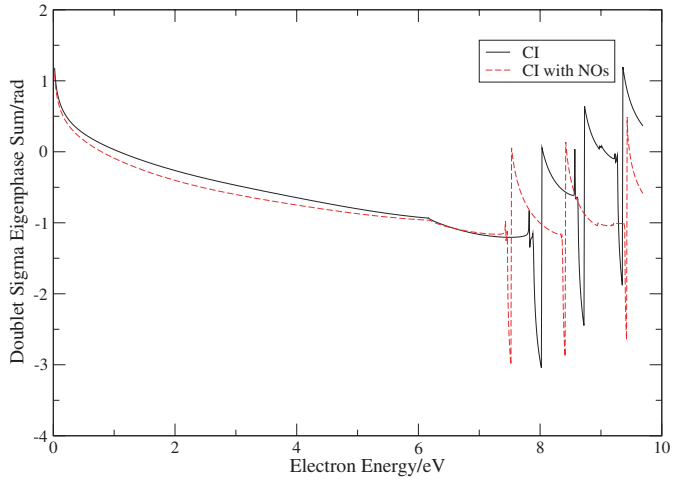

Figure 3. Comparison of HNC $^2\Sigma^+$ eigenphase sum curves for the basis set 6-31G.

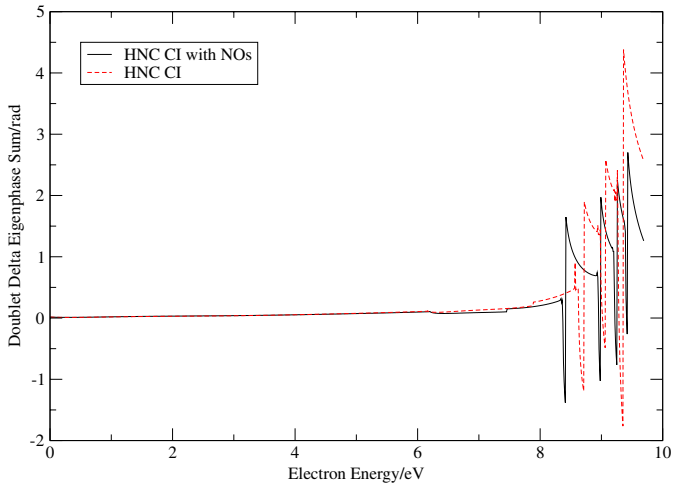

Figure 4. Comparison of HNC $^2\Delta$ eigenphase sum curves for the basis set 6-31G.

polarization) predict Feshbach resonances of both $^2\Sigma^+$ and $^2\Delta$ symmetry is hardly surprising since the two resonances both arise from the addition of a σ electron to target states with the same configuration ($1\sigma^2 2\sigma^2 3\sigma^2 4\sigma^2 5\sigma^2 1\pi^3 2\pi^1$), these resonances therefore probably both have the same configuration: $1\sigma^2 2\sigma^2 3\sigma^2 4\sigma^2 5\sigma^2 1\pi^3 2\pi^1 6\sigma^1$.

Two of our models found a further, narrow $^2\Sigma^+$ resonance at 9.2 eV. However, we cannot be confident that our study gives stable results at this energy given the uncertainties in the target state calculations.

Figures 3 and 4 show the $^2\Sigma^+$ and $^2\Delta$ eigenphases. Both are similar to those of HCN (whose $^2\Delta$ eigenphase is not shown) below the excitation thresholds. Above these thresholds the eigenphases display considerable structure.

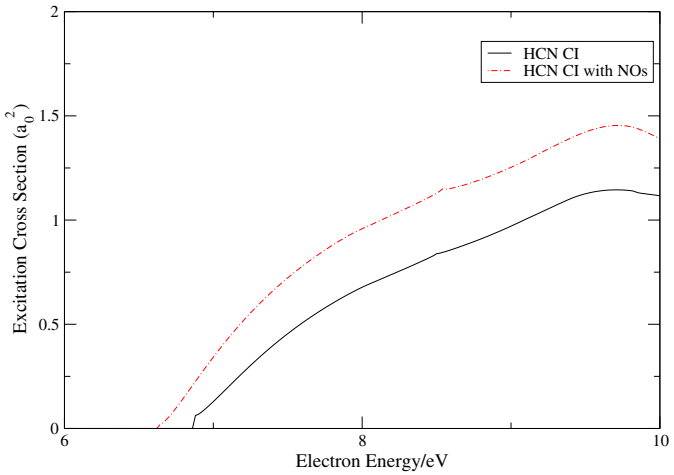

Figure 5. HCN electron impact excitation cross-section for $X^1\Sigma^+ \rightarrow 1^3\Sigma^+$.

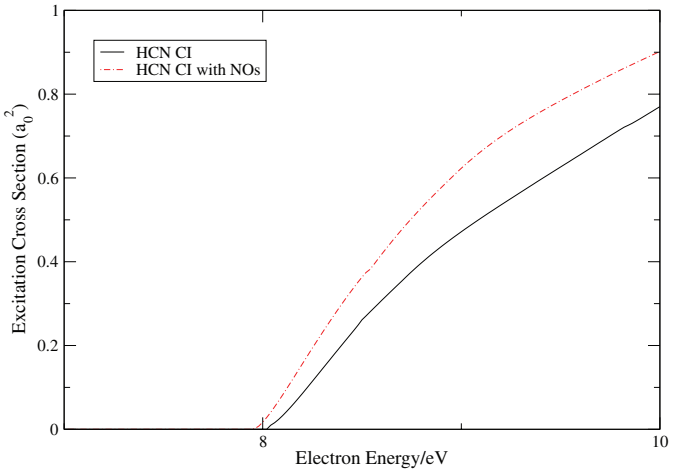

Figure 6. HCN electron impact excitation cross-section for $X^1\Sigma^+ \rightarrow 1^3\Delta$.

4.3. Electronic excitation

Electron impact electronic excitation of either HCN or HNC does not appear to have been considered previously. Figures 5–8 give electron impact excitation cross-sections for excitation to the lowest two excited states of HCN and HNC, respectively. The cross-sections presented were all calculated using the 6-31G GTO basis and uncontracted virtual orbital CSFs. However, the main variation between models in the magnitude of the calculated excitation cross-sections in the near-threshold region studied is due to location of the excitation threshold. Therefore the resonance energy position is determined by the quality of the target calculation rather than any details of the scattering model used. In all figures the differences between full and dashed curves can be thought of as approximately representing the degree of uncertainty in our calculations.

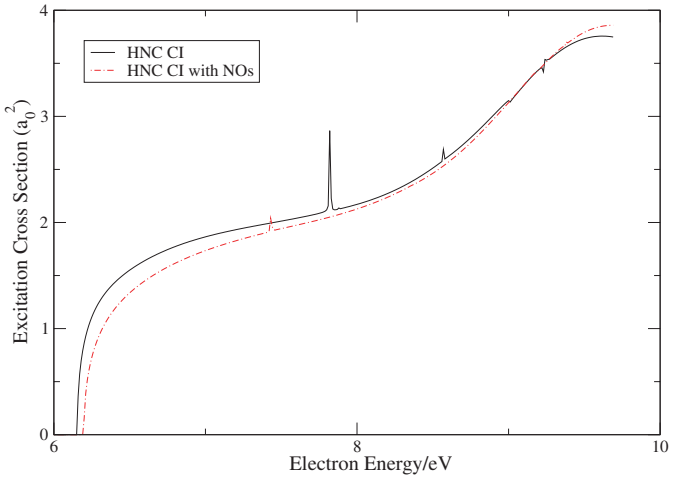

Figure 7. HNC electron impact excitation cross-section for $X^1\Sigma^+ \rightarrow 1^3\Pi$.

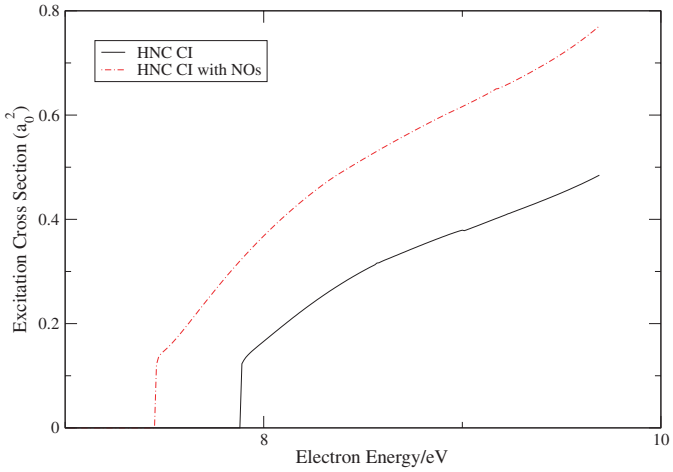

Figure 8. HNC excitation cross-section curves $X^1\Sigma^+ \rightarrow 1^3\Sigma^+$.

5. Conclusion

We have applied the *R*-matrix method to electron scattering by HCN and HNC. The present work represents the first study of electron scattering by the latter molecule. 24 target states were included in the scattering calculation and were represented by CI wavefunctions, which in our best model, were subsequently improved by the use of pseudo natural orbitals. We detect an $HCN^-\ ^2\Pi$ shape resonance in our models. This resonance is well known both experimentally (Srivastava *et al* 1978, Edard *et al* 1990, Burrow *et al* 1992) and theoretically (Jain and Norcross 1985, 1986). Our resonance positions are in reasonable agreement with previous studies. The resonance width does not appear to have been determined experimentally and our calculations suggest that the width is somewhat narrower than that predicted by Jain and Norcross. Indeed, as resonances tend to narrow as the treatment of polarization effects is

improved, we would actually expect that our narrowest width, 1.14 eV, probably represents an upper limit on the true width.

Electron collision calculations on the linear isomer HNC find that there is also $HNC^- \, ^2\Pi$ shape resonance at an energy similar to its HCN^- counterpart. However, we find that the HNC^- shape resonance is some 40% narrower than the HCN^- one. Unlike HCN, HNC appears to support a number of Feshbach resonances. In particular our better calculations found narrow resonances of $^2\Sigma^+$ and $^2\Delta$ symmetry lying less than 0.1 eV below the first excited states of $^3\Sigma^+$ and $^3\Delta$ symmetry, respectively. These resonances probably both arise from the same configuration: $1\sigma^2 2\sigma^2 3\sigma^2 4\sigma^2 5\sigma^2 1\pi^3 2\pi^1 6\sigma^1$.

Coupled-state electron scattering calculations such as these contain a wealth of information on various different scattering processes. We present results on electron impact electronic excitation of both isomers and plan, in future work, to study electron impact rotational excitation rates which are of particular importance in astrophysics (Lovell *et al* 2004). Elastic and inelastic cross-sections for other processes discussed in the present paper are available from the authors.

Finally we have taken the opportunity to compare our results with those obtained by the new Quantemol-N *R*-matrix expert system. In general this code gives very similar results to those obtained using the standard UK Molecular *R*-matrix code. The most important difference, which gives rise to slightly higher positions for the shape resonances, is the reduced number of target states used by Quantemol-N in its default mode.

Acknowledgments

HNV is indebted to PPARC for the provision of a CASE studentship. We also thank R Chaudhuri and S Krishnamachari for providing their HCN adiabatic excitation energy data and I Rozum, A Faure and KL Baluja for useful discussions.

References

Burke P G and Berrington K A 1993 *Atomic and Molecular Processes—An R-matrix Approach* (Bristol: Institute of Physics Publishing)
Burke P G and Tennyson J 2005 *Mol. Phys.* **103** 2537–48
Burrow P D, Howard A E, Johnston A R and Jordan K D 1992 *J. Phys. Chem.* **96** 7570–8
Edard F, Hitchcock A P and Tronc M 1990 *J. Phys. Chem.* **94** 2768–74
Faure A, Gorfinkiel J D, Morgan L A and Tennyson J 2001 *Comput. Phys. Commun.* **144** 224–41
Frisch M J *et al* 2004 *Gaussian 03* (Revision C.02) (Wallingford, CT: Gaussian Inc.)
Gil T J, Lengsfield B H, Mc Curdy C W and Rescigno T N 1994 *Phys. Rev.* A **49** 2551–60
Gorfinkiel J D and Tennyson J 2004 *J. Phys. B: At. Mol. Opt. Phys.* **37** L343–50
Gorfinkiel J D and Tennyson J 2005 *J. Phys. B: At. Mol. Opt. Phys.* **38** L1607–1622
Harris G J, Pavlenko Ya V, Jones H R A and Tennyson J 2003 *Mon. Not. R. Astron. Soc.* **344** 1107–18
Herzberg G 1966 *Electronic Spectra and Electronic Structure of Polyatomic Molecules* (New York: Van Nostrand Reinhold)
Hirota T, Yamamoto S, Mikami H and Ohishi M 1998 *Astrophys. J.* **503** 717–28
Jain A and Norcross D W 1985 *Phys. Rev.* A **32** 134–43
Jain A and Norcross D W 1986 *J. Chem. Phys.* **84** 739–44
Jimenez-Serra I, Martin-Pintado J, Viti S, Martin S, Rodriguez-Franco A, Faure A and Tennyson J 2006 *Astrophys. J.* **650** L135–8
Krishnamachari S N L G and Venkatsubramanian R 1986 *Spectrosc. Lett.* **19** 55
Lovell A J, Kallivayalil N, Schloerb G P, Combi M R, Hansen K C and Gombosi T I 2004 *Astrophys. J.* **613** 615–21
Morgan L A, Gillan C J, Tennyson J and Chen X 1997 *J. Phys. B: At. Mol. Opt. Phys.* **30** 4087–96
Morgan L A, Tennyson J and Gillan C J 1998 *Comput. Phys. Commun.* **114** 120–8
Munjal H and Baluja K L 2006 *Phys. Rev.* A **74** 032712

Nayak A K, Chaudhuri R K and Krishnamachari S N L G 2005 *J. Chem. Phys.* **122** 184323
NIST 2005 http://srdata.nist.gov/cccbdb/ and references therein
Rozum I, Mason N J and Tennyson J 2003 *New J. Phys.* **5** 155
Salvini S, Burke P G and Noble C J 1984 *J. Phys. B: At. Mol. Opt. Phys.* **17** 2549–61
Schwenzer G M, O'Neil S V, Schaefer H F, Baskin C P and Bender C F 1974 *J. Chem. Phys.* **60** 2787–93
Schwenzer G M, Schaefer H F and Bender C F 1975 *J. Chem. Phys.* **63** 569–72
Skurski P, Gutowski M and Simons J 2001 *J. Chem. Phys.* **114** 7443–9
Srivastava S K, Tanaka H and Chutjian A 1978 *J. Phys. Chem.* **69** 1493–7
Tennyson J 1996 *J. Phys. B: At. Mol. Opt. Phys.* **29** 6185–201
Tennyson J and Noble C J 1984 *Comput. Phys. Commun.* **33** 421–4
Tennyson J and Morgan L A 1999 *Phil. Trans. R. Soc.* A **357** 1161–73
Tennyson J, Brown D B, Munro J J, Rozum I, Vinci N and Varambhia H N 2006 *Quantemol-N version 2.3.3* www.quantemol.com
Van Mourik T, Harris G J, Polyansky O L, Tennyson J, Csaszar A G and Knowles P J 2001 *J. Chem. Phys.* **115** 3706–18